Electronic Supplementary Information to

Imaging of nanoparticle uptake and kinetics of intracellular trafficking in individual cells

by N. Vtyurina et al.

Supplementary Methods

Cell Culture

HeLa and HeLa Kyoto cells were subcultured 1:3 every second or third day by incubating them in 0.25% trypsin for 3 min when they were confluent. HeLa cells were cultured in Minimum Essential Medium (MEM) supplemented 10% fetal bovine serum (FBS) and HeLa Kyoto cells in Dulbecco's modified Eagle's medium (DMEM) supplemented with 10% FBS, allowing growth up to a maximum of 20 passages after defrosting. Regular monthly mycoplasma tests were carried out, confirming cells were mycoplasma free. Cells were cultured at 37 °C and 5% CO_2 in reagents purchased from Gibco (Thermo Fisher Scientific) unless otherwise specified.

Nanoparticles

Nanoparticle size (hydrodynamic diameter) was determined using a Malvern Zetasizer Nano Series. Carboxylated polystyrene nanoparticles from Invitrogen (Thermo Fisher Scientific) were diluted to a final concentration of 75 µg/ml (for 40 nm), 300 µg/ml (for 100 nm) or 1600 µg/ml (for 200 nm) in complete MEM cell culture medium supplemented with 4 mg/ml human serum (human serum from pooled donors, TCS BioSciences) and immediately measured (or added to cells). The results are the average and standard deviation over three separate measurements of the same dispersions.

Expression of fluorescent protein constructs and staining

In addition to the constructs and staining indicated in the main manuscript, the following constructs in mammalian expression vectors were received as gifts as indicated: the ctEEA1-GFP plasmid was obtained from the O. Bakke's lab (Department of Molecular Biosciences, University of Oslo);[1] pMyrPaln-mEGFP[2] (Addgene plasmid #21038) was a gift from D. Gerlich (Institute of Molecular Biotechnology of the Austrian Academy of Sciences, Vienna BioCenter); Lamp1-RFP[3] (Addgene plasmid #1817) was a gift from W. Mothes (Department of Microbial Pathogenesis, Yale University School of Medicine, New Haven). Typically, 30,000 cells were seeded for imaging on 4-well 35 mm petri dishes (Greiner Bio-One) allowing tracking of several conditions simultaneously. 20 h after seeding, cells were treated with FuGene transfection reagent (Promega) and 0.02 µg/µl DNA using the manufacturer's protocol. After 20 h, cells were washed and subsequently exposed to nanoparticles. Transfected cells were detected by GFP- or RFP fluorescence.

Image acquisition

Dual color visualization of cells was performed using a DeltaVision Elite fluorescence microscope (GE Healthcare) equipped with a PCO-edge sCMOS camera and solid state illumination, and a Laser Scanning Confocal Microscope LSM880 (Zeiss)

equipped with an Airyscan detector. LSM880 images were acquired in fast airy scan mode. Both microscopes had a motorized xy stage allowing to record images over time in different positions in the sample and a piezo stepper for fast z-sectioning. Images were acquired with a 100x oil NA = 1.45 (DeltaVision) or 63x glycerol/oil NA = 1.2 (LSM880) immersion objectives. Yellow-green nanoparticles and GFP were excited at 488 nm, and red nanoparticles and RFP at 561 nm. For each fluorescence channel, consecutive three-dimensional (3D) images (z-stacks) of 25-30 optical sections were acquired with focal planes 0.30 µm apart. 3D z-stacks of 5-20 whole volume individual cells were recorded simultaneously every 10-20 min for up to 6 h. DeltaVision images were subsequently deconvoluted using the SoftWoRx software (Applied Precision Ltd.).

The majority of data were acquired with the LSM880 confocal microscope, except the data presented in Fig. 6D, Supplementary Figs. S2-4, S13B-E and Supplementary Movies S6-7, which were acquired with the DeltaVision microscope.

Image processing and colocalization data analysis

Data was analyzed using Imaris 7.6.4 software (Bitplane). Briefly, the channel for the protein or LysoTracker marker was used to determine cell borders manually. Based on these borders, a 3D mask of the full cell was generated with the “Surface” algorithm defining a three-dimensional region of interest (ROI) excluding nanoparticles outside of the cell. For HeLa Kyoto cells the same mask was applied over all time points to the fluorescence channels of both the protein/LysoTracker marker and of the nanoparticles, thanks to low or absence of cell displacement. For HeLa cells, due to substantial cell displacement over time, cell borders were defined for each time point and then masks were applied to the fluorescence channels of both the protein/ LysoTracker marker and nanoparticles. For each individual cell, the volume and the surface area of the generated mask was calculated by Imaris. For HeLa Kyoto cells these parameters remained roughly constant over time, while for HeLa they varied. Thus, to present a single volume/surface area for a given cell, the results were averaged over all the recorded time points.

For each ROI and channel, based on the mean intensity of the signal, images were segmented using the “Spot detection” algorithm with automatic background subtraction. Homogeneous spherical objects with fixed volume were created with diameters of 0.2 µm, 0.4 µm 0.5 µm for 40, 100 and 200 nm nanoparticles respectively and 0.5 µm for lysosomes, 0.3 µm for clathrin, 0.4 µm for caveolin-1 and early endosomes (Rab5). Note that images are diffraction-limited and these sizes consequently do not represent the real physical sizes. The identified objects were classified and filtered using the mean intensity filter and by manually setting up thresholds based on visual inspection of the created objects in correspondence with the raw signal from the image. Note that what was identified as a nanoparticle "object" may contain several nanoparticles too close together to be resolved optically.

In order to quantify the nanoparticle objects colocalized with the protein/LysoTracker objects of interest, the Imaris Matlab function “Colocalize spots” was used. A nanoparticle object was determined to be colocalized with the protein/LysoTracker object if their centers were a maximum of 0.5 µm apart (Visual inspection of the images confirmed that this allowed to identify colocalized objects appropriately) The number of nanoparticle objects, protein/LysoTracker objects and colocalized nanoparticle

objects were calculated applying the same set of parameters over all recorded time points and across all data sets. The fraction of colocalized nanoparticle objects was calculated as the ratio between the number of colocalized nanoparticle objects and all cell-associated nanoparticle objects at each time point. 5-20 individual cells were acquired for each condition, as specified in the captions.

When restricting the analysis only to objects closer to the cell membrane (Fig. 6), the borders of the interior of each cell were manually defined based on the protein marker fluorescence in order to exclude the perinuclear region where usually large clusters of lysosomes are present and in which the excess fluorescent marker accumulates for degradation. Based on these borders, 3D masks were generated using the “Surface” algorithm and the volume generated was excluded from the analysis. Then, nanoparticle and protein objects were identified and the colocalization algorithm was applied as described above.

The time-lapse records of HeLa Kyoto cells expressing labelled clathrin or Rab5 shown in Fig. 6D were acquired with DeltaVision Elite, recording a 3D stack every 10 min, after which the images were deconvoluted and analyzed with Imaris as described above.

For the data shown in Supplementary Figs. S2-S3, raw images acquired with DelatVision Elite were masked based on the channel for the protein marker. Cell borders were defined manually to select a 3D ROI, excluding nanoparticles outside of the cell. The ImageJ tool DiAna was used for object-based 3D colocalization.[4] Parameters for image segmentation were set for each channel separately based on visual inspection of the created objects and correspondence with the raw signal from the image. Then the number of overlapped objects in each channel was used to calculate the fraction of colocalized nanoparticle objects as described above.

Statistical analysis

Statistical analysis of kinetic parameters evaluated from single cells (Fig. S10) was carried out using non-parametric rank-based methods and a significance level of 5%. A Mann-Whitney test was used to assess differences between the two HeLa cell types, while a Kruskal-Wallis test was used to assess differences between the three nanoparticle sizes. In the latter case, when results were significantly different, a Conover pairwise multiple comparison test was performed to identify the samples that differed. The analysis was performed in R version 3.6.3, using the PMCMR package version 1.9.0 for pairwise multiple comparisons.

Diameter (nm)	40	100	200
Mass concentration (µg/ml)	75	300	1600
Molar concentration (nM)	3.5	0.91	0.60
Number protein adsorption sites/particle	200	1300	5000
Molar concentration adsorption sites (µM)	0.7	1.1	3.0
Ratio molar concentration protein/adsorption sites	85	53	20

Supplementary Table S1. Nanoparticle and protein concentrations. The experiments were performed with a known mass concentration of nanoparticles (stemming from the manufacturer). To convert the mass concentration into a molar concentration, we used the nominal diameter (also given by the manufacturer) and a polystyrene density of 1.05 g/ml. The nanoparticles were suspended in 4 mg/ml of human serum. In order to convert this concentration into molar concentration, one must in principle know the abundance and molar weight of each species; since this is not available, we considered human serum albumin as a "typical protein". Human serum albumin is the most abundant protein in human serum and has a molecular weight of 66.5 kDa. Assuming this to be the molecular weight of a "typical protein", 4 mg/ml of serum corresponds to a molar concentration of 60 µM. To estimate the number of proteins that can adsorb to the nanoparticle surface, we note that literature suggests that when human serum albumin adsorbs to polymer-coated FePt nanoparticles, its occupied surface area forms an equilateral triangle with 8 nm sides,[5] implying an area of 27 nm^2. As a comparison, the surface area occupied by transferrin has been estimated to be 42 nm^2 and 66 nm^2 on polymer-coated FePt[6] and on polystyrene[7] nanoparticles, respectively. As the occupied surface area of a "typical protein" we thus take 25 nm^2, which likely leads to an *over*estimate of the number of proteins that can fit on a particle. With this estimate we can then calculate the molar concentration of protein adsorption sites. Such a calculation shows that the number of proteins is in clear excess of the number of adsorption sites.

Sample	Medium	Diameter (z-average, nm)	PDI*	Diameter (nm)
PS-COOH nanoparticles 40 nm	PBS	49±1	0.05±0.02	-
	hsMEM	-	-	136±8
PS-COOH nanoparticles 100 nm	PBS	108±1	0.01±0.01	-
	hsMEM	-	-	178±1
PS-COOH nanoparticles 200 nm	PBS	168±3	0.02±0.03	-
	hsMEM	-	-	247±6

*** Polydispersity index (PDI)**

Supplementary Table S2. Nanoparticle characterization. Diameter (z-average, nm) and polydispersity index (PDI) obtained by cumulant analysis and diameter (nm) obtained by CONTIN analysis of data of fluorescent nanoparticle dispersions in phosphate buffered saline (PBS) and in MEM supplemented with 4 mg/ml human serum (hsMEM) measured at 20°C. Dispersions to a final concentration of 75 µg/ml (for 40 nm), 300 µg/ml (for 100 nm) or 1600 µg/ml (for 200 nm) in hsMEM cell culture medium were prepared and measured after dispersion. The results are the average and standard deviation over three separate measurements of the same dispersions. The corresponding size distributions are shown in Supplementary Figure S1.

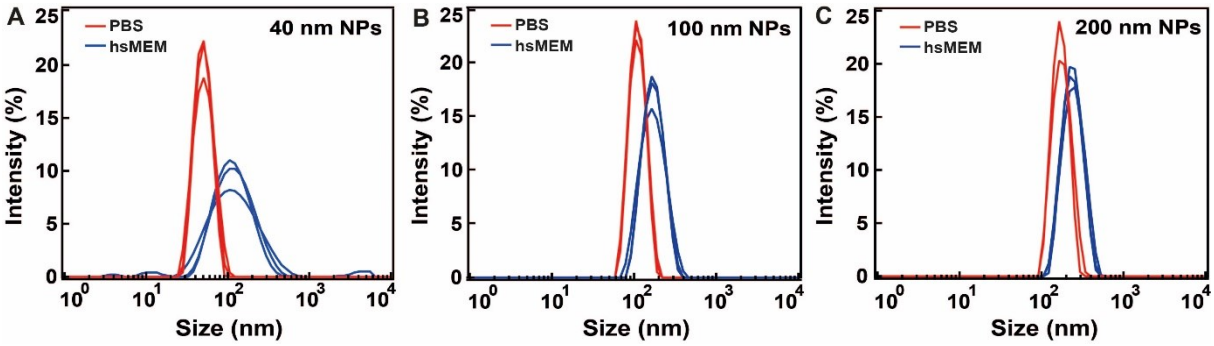

Supplementary Figure S1. Nanoparticle characterization. Comparison of the size distributions obtained by DLS for ***(A)*** 75 µg/ml 40 nm nanoparticles, ***(B)*** 300 µg/ml 100 nm nanoparticles and ***(C)*** 1600 µg/ml 200 nm nanoparticles in PBS *(red)* and MEM supplemented with 4 mg/ml human serum (hsMEM) *(blue)*. The results of 3 replicate measurements of the same dispersion are shown.

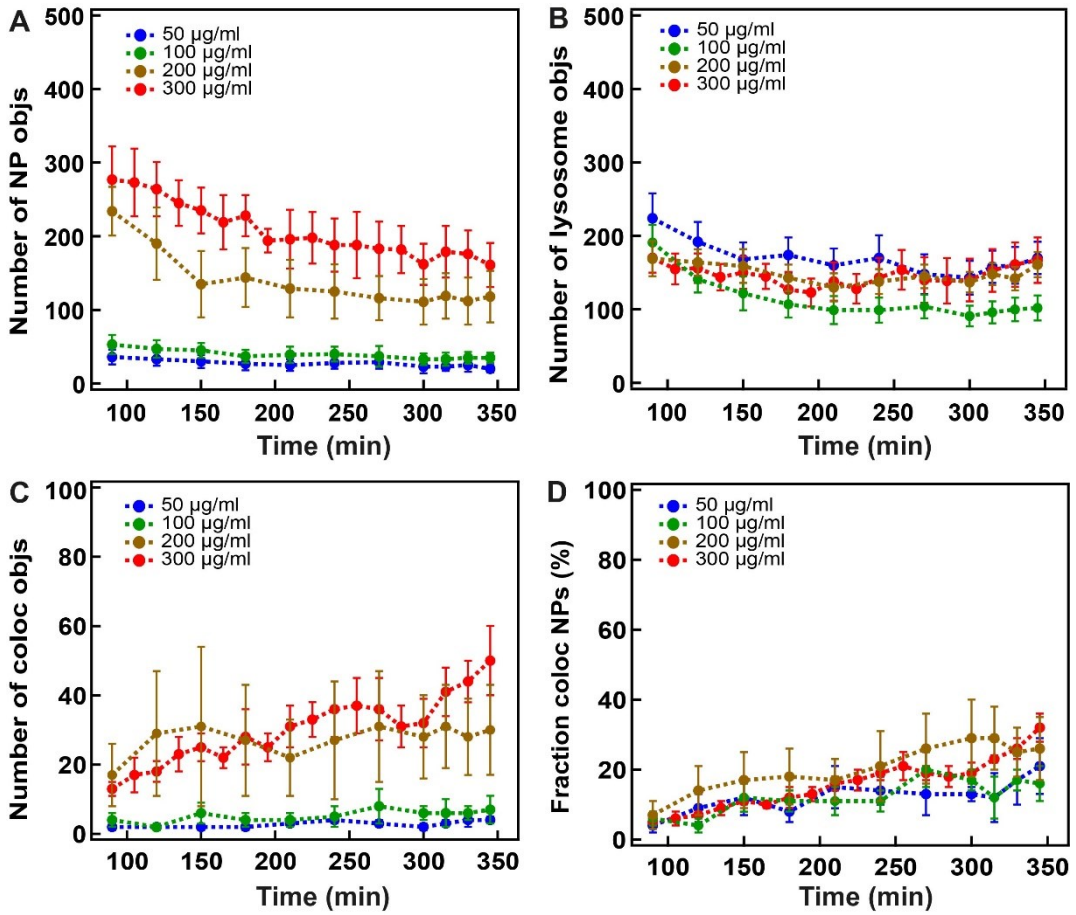

Supplementary Figure S2. Nanoparticle colocalization with lysosomes after exposure to different nanoparticle doses. HeLa cells were exposed for a 10 min "pulse" to different doses of 40 nm carboxylated polystyrene nanoparticles and then cells were "chased" as described in the Experimental section. The results are presented as averages and standard error over 8 individual cells (Mean± SE (n=8)). *(A)* Average number of detected nanoparticle objects. *(B)* Average number of detected lysosome objects. *(C)* Average number of colocalized nanoparticle objects. *(D)* Average fraction of colocalized nanoparticle objects. z-stacks were acquired with a DeltaVision Elite. The results showed that the fraction of colocalized nanoparticle object was comparable in cells exposed to different nanoparticle doses. We note that for this dataset, the fraction of colocalized nanoparticle objects was calculated using ImageJ as described in the Supplementary Methods and, probably because of the different method used, it was overall lower than what is shown in Fig. 4. No major differences in the fractions of colocalized nanoparticle objects (*D*) were observed when exposing cells to different doses of nanoparticles.

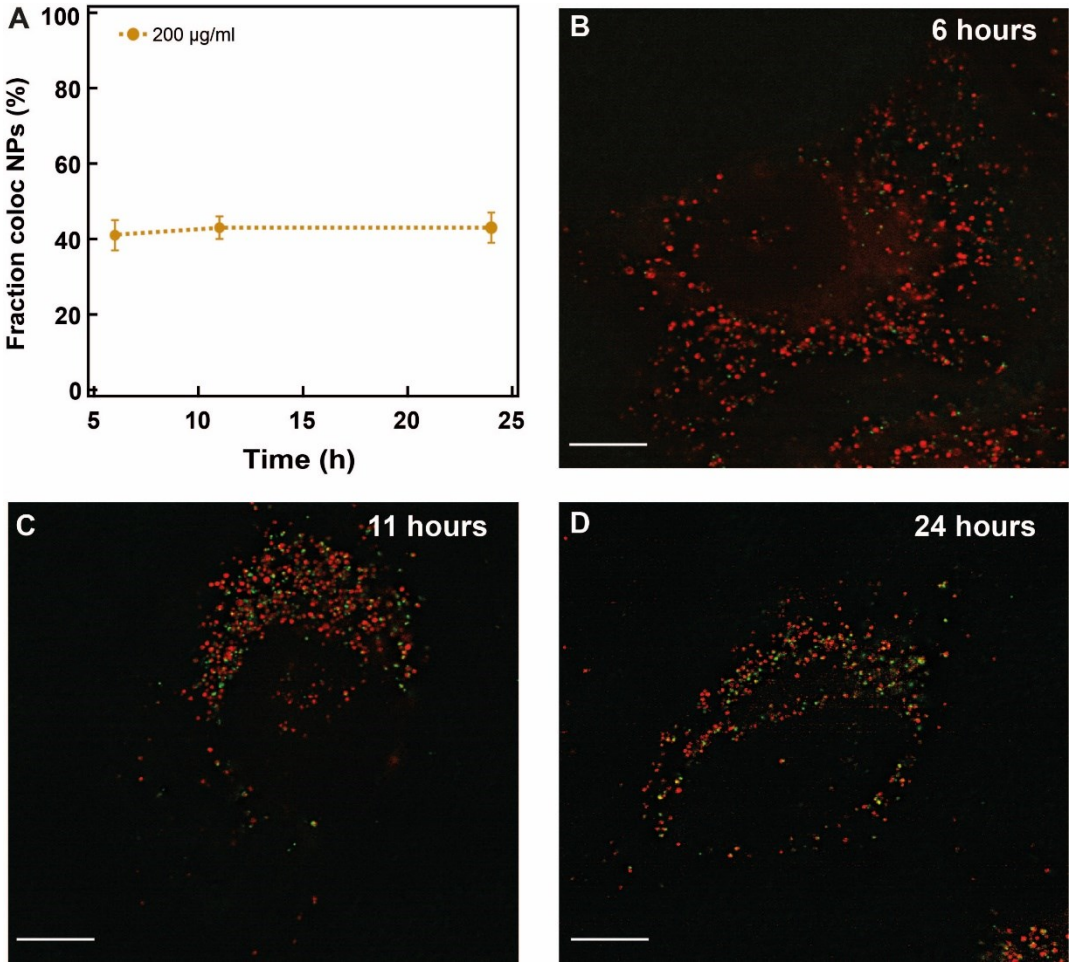

Supplementary Figure S3. Nanoparticle colocalization with lysosomes up to 24 h "chase". HeLa cells were exposed for a 10 min "pulse" of 200 µg/ml 40 nm carboxylated polystyrene nanoparticles and then cells were "chased" as described in the Experimental section *(A)* Fraction of colocalized nanoparticle objects averaged over cells (Mean± SE (n=8)). *(B-D)* Representative images (acquired with DeltaVision and deconvoluted) of HeLa cells exposed to 200 µg/ml of 40 nm nanoparticles *(green)* and labeled with LysoTracker *(red)* after a "chase" of 6 h *(B)*, of 11 h *(C)* and of 24 h *(D)*. Scale bar 10 µm. The fraction of colocalized nanoparticle objects did not increase further even after a 24 h chase.

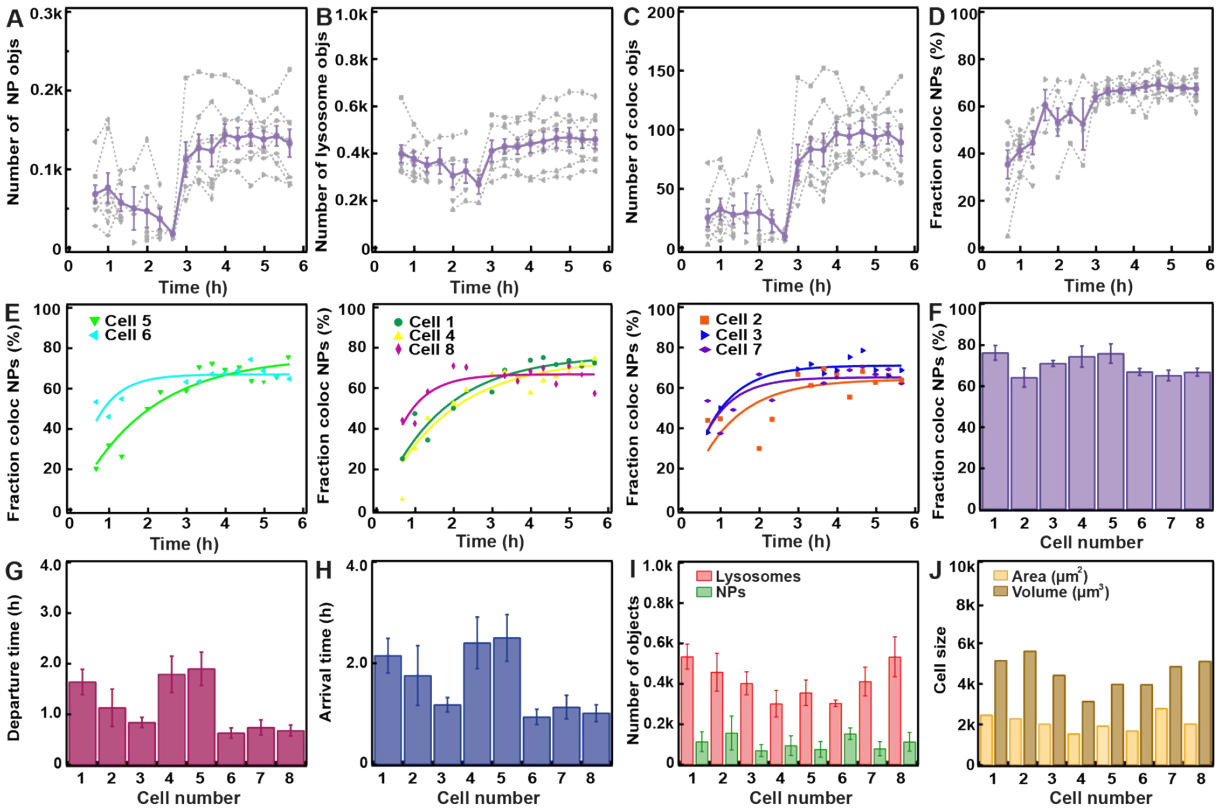

Supplementary Figure S4. Nanoparticle colocalization with lysosomes in HeLa Kyoto cells exposed for 5 min to 75 µg/ml 40 nm nanoparticles in DMEM medium supplemented with 4 mg/ml human serum and stained with LysoTracker. Average number over all cells *(light purple)* and for individual cells *(grey)* of ***(A)*** detected nanoparticle objects, ***(B)*** lysosome objects, ***(C)*** nanoparticle objects colocalized with lysosome objects and ***(D)*** fraction of nanoparticle objects colocalized with lysosome objects. The average results are the mean and standard error of the results obtained in 8 individual cells. ***(E)*** Fits of Eq. 2 *(solid line)* to the fraction of nanoparticle objects colocalized with lysosome objects *(symbols)* in individual cells. ***(F)*** Fraction of nanoparticle objects ultimately colocalized with lysosome objects (f_l) extracted from the fits to individual cells shown in E. ***(G)*** Departure time of nanoparticle objects from the membrane (τ) extracted from the fits to individual cells shown in E. ***(H)*** Lysosome arrival time of nanoparticle objects (τ_l) calculated from F and G. Error bars in panel F, G are uncertainties from the fit, while error bars in panel H are uncertainties propagated from those of f_l and τ using Gauss' formula. ***(I)*** Number of nanoparticle *(red)* and lysosome objects *(green)* detected in individual cells averaged over all time points. The average results are the mean and standard error of the results obtained over 16 time points. ***(J)*** Area *(yellow)* and volume *(brown)* of individual cells. z-stack images were acquired using a Zeiss LSM 880. We note that in the first 2.5 h (panels A-C), we observed unusual variations in the number of detected objects for both channels at different time points due to technical issues of the instrument (likely unstable exposure settings during the automated measurements). This resulted in varying intensity values in the recorded images. Because of the variation in the image intensity, the analysis gave an apparent decrease in the number of objects identified in the first 2.5 h (panels A-C). However, visual inspection of the raw images showed that no sudden changes in the objects inside cells occurred. As this technical issue does not affect the overall results for the fraction of colocalized nanoparticle objects (panel D), all images acquired have been analyzed with the same parameters and threshold values across all recorded time points.

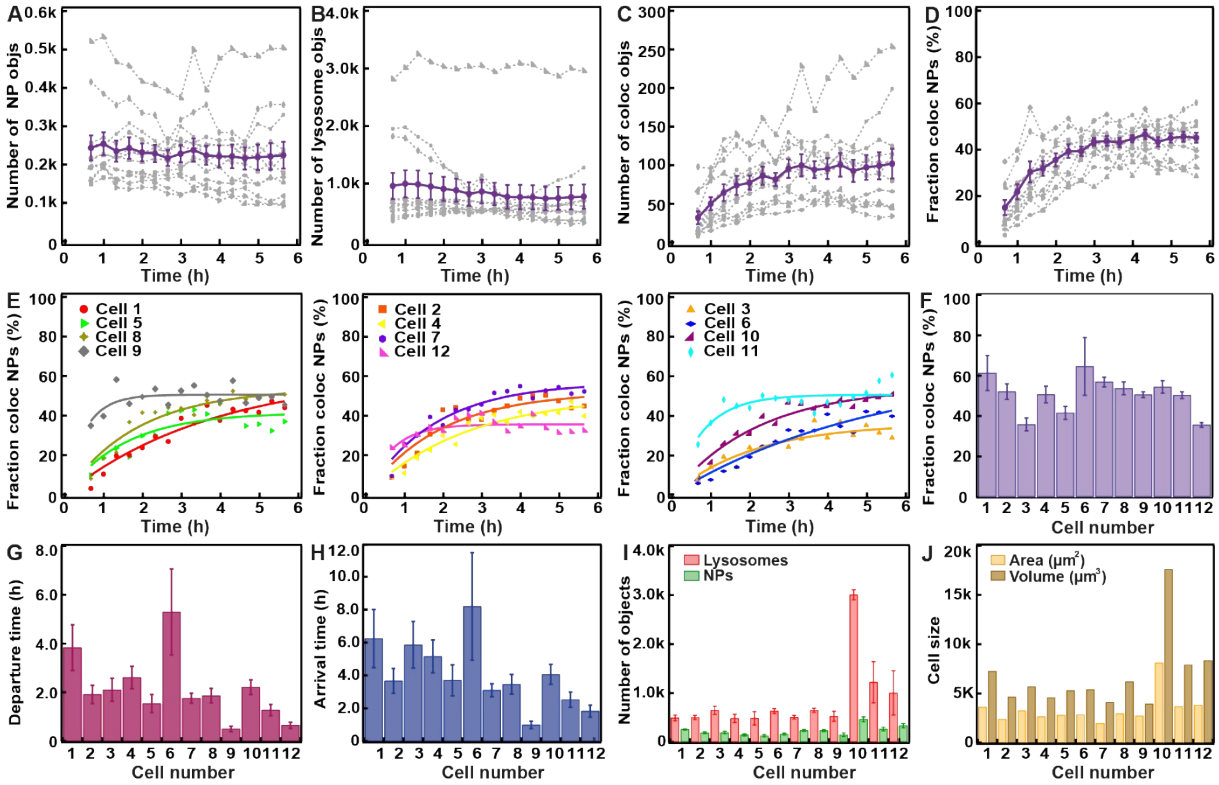

Supplementary Figure S5. Nanoparticle colocalization with lysosomes in HeLa Kyoto cells exposed for 10 min to 300 µg/ml 100 nm nanoparticles in DMEM medium supplemented with 4 mg/ml human serum and stained with LysoTracker. Average number over all cells *(purple)* and for individual cell *(grey)* of *(**A**)* detected nanoparticle objects, ***(B)*** lysosome objects, ***(C)*** nanoparticle objects colocalized with lysosome objects and ***(D)*** fraction of nanoparticle objects colocalized with lysosome objects. The average results are the mean and standard error of the results obtained in 12 individual cells. ***(E)*** Fits of Eq. 2 *(solid line)* to the fraction of nanoparticle objects colocalized with lysosome objects *(symbols)* in individual cells. ***(F)*** Fraction of nanoparticle objects ultimately colocalized with lysosome objects (f_l) extracted from the fits to individual cells shown in E. ***(G)*** Departure time of nanoparticle objects from the membrane (τ) extracted from the fits to individual cells shown in E. (***H)*** Lysosome arrival time of nanoparticle objects (τ_l) calculated from F and G. Error bars in panel F, G are uncertainties from the fit, while error bars in panel H are uncertainties propagated from those of f_l and τ using Gauss' formula. ***(I)*** Number of nanoparticle *(red)* and lysosome objects *(green)* detected in individual cells averaged over all time points. The average results are the mean and standard error of the results obtained over 16 time points. ***(J)*** Area *(yellow)* and volume *(brown)* of individual cells. z-stack images were acquired using a Zeiss LSM 880.

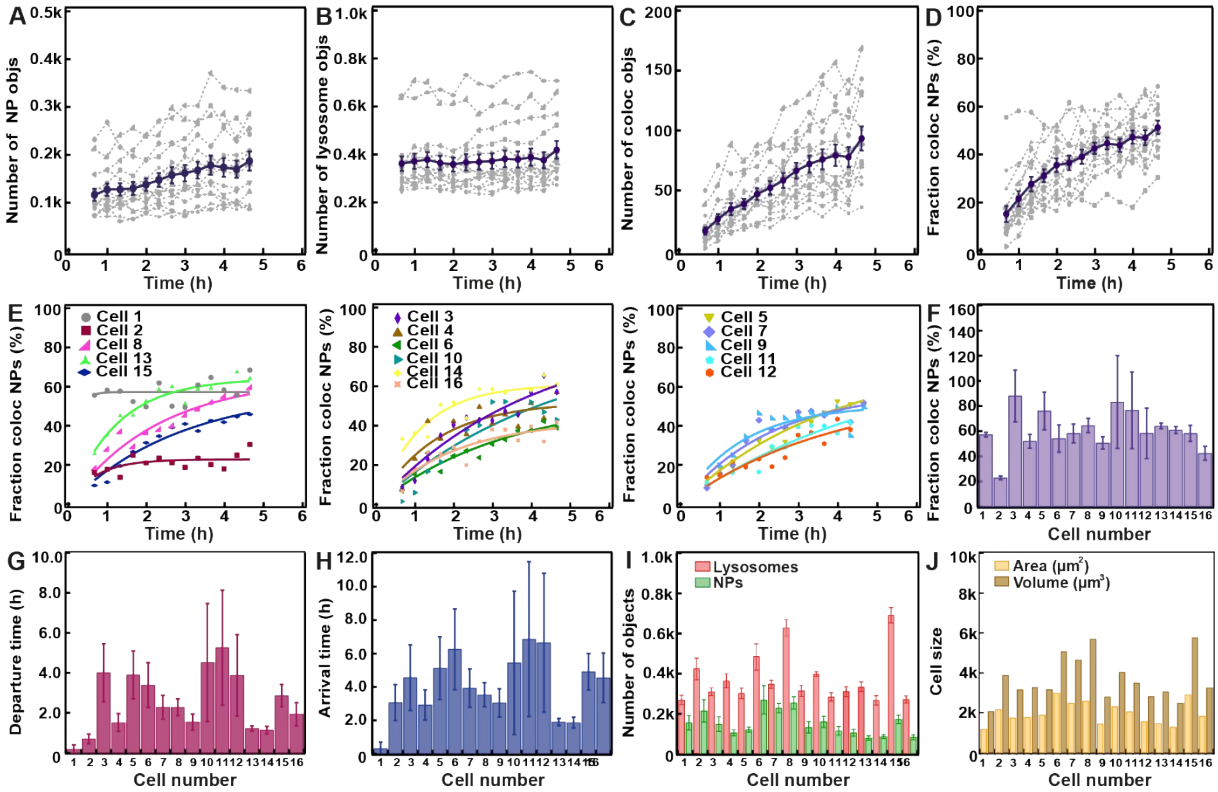

Supplementary Figure S6. Nanoparticle colocalization with lysosomes in HeLa Kyoto cells exposed for 15 min to 1600 µg/ml 200 nm nanoparticles in DMEM medium supplemented with 4 mg/ml human serum and stained with LysoTracker. Average number over all cells *(dark purple)* and for individual cells *(grey)* of ***(A)*** detected nanoparticle objects, ***(B)*** lysosome objects, ***(C)*** nanoparticle objects colocalized with lysosome objects and ***(D)*** fraction of nanoparticle objects colocalized with lysosome objects. The average results are the mean and standard error of the results obtained in 16 individual cells. ***(E)*** Fits of Eq. 2 *(solid line)* to fraction of nanoparticle objects colocalized with lysosome objects *(symbols)* in individual cells. ***(F)*** Fraction of nanoparticle objects ultimately colocalized with lysosome objects (f_l) extracted from the fits to individual cells shown in E. ***(G)*** Departure time of nanoparticle objects from the membrane (τ) extracted from the fits to individual cells shown in E. ***(H)*** Lysosome arrival time of nanoparticle objects (τ_l) calculated from F and G. Error bars in panel F, G are uncertainties from the fit, while error bars in panel H are uncertainties propagated from those of f_l and τ using Gauss' formula. ***(I)*** Number of nanoparticle *(red)* and lysosome objects *(green)* detected in individual cells averaged over all time points. The average results are the mean and standard error of the results obtained over 13 time points. ***(J)*** Area *(yellow)* and volume *(brown)* of individual cells. z-stack images were acquired using a Zeiss LSM 880.

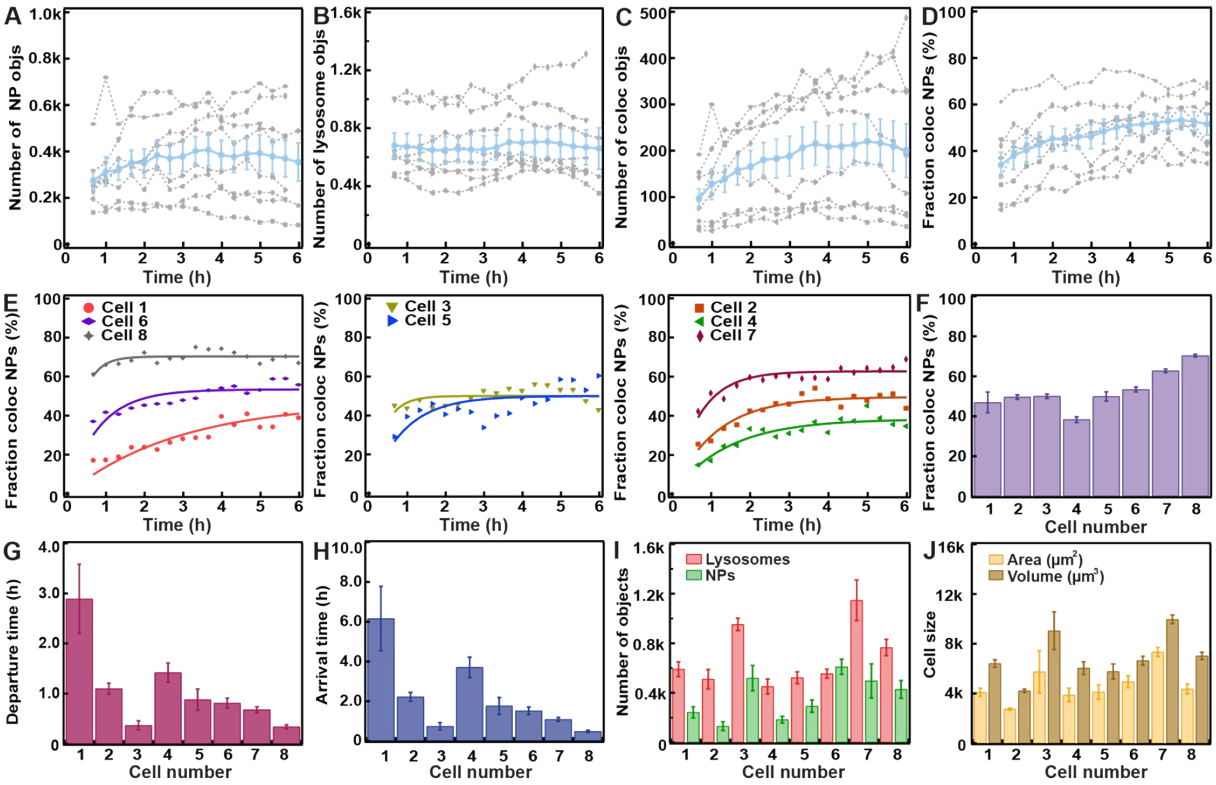

Supplementary Figure S7. Nanoparticle colocalization with lysosomes in HeLa cells exposed for 5 min to 75 µg/ml 40 nm nanoparticles in DMEM medium supplemented with 4 mg/ml human serum and stained with LysoTracker. Average number over all cells *(light blue)* and for individual cells *(grey)* of ***(A)*** detected nanoparticle objects, ***(B)*** lysosome objects, ***(C)*** nanoparticle objects colocalized with lysosome objects and ***(D)*** fraction of nanoparticle objects colocalized with lysosome objects. The average results are the mean and standard error of the results obtained in 8 individual cells. ***(E)*** Fits of Eq. 2 *(solid line)* to the fraction of nanoparticle objects colocalized with lysosome objects *(symbols)* in individual cells. ***(F)*** Fraction of nanoparticle objects ultimately colocalized with lysosome objects (f_l) extracted from the fits to individual cells shown in E. ***(G)*** Departure time of nanoparticle objects from the membrane (τ) extracted from the fits to individual cells shown in E. (***H)*** Lysosome arrival time of nanoparticle objects (τ_l) calculated from F and G. Error bars in panel F, G are uncertainties from the fit, while error bars in panel H are uncertainties propagated from those of f_l and τ using Gauss' formula. ***(I)*** Number of nanoparticle *(red)* and lysosome objects *(green)* detected in individual cells averaged over all time points. The average results are the mean and standard error of the results obtained over 16 time points. ***(J)*** Area *(yellow)* and volume *(brown)* of individual cells. z-stack images were acquired using a Zeiss LSM 880.

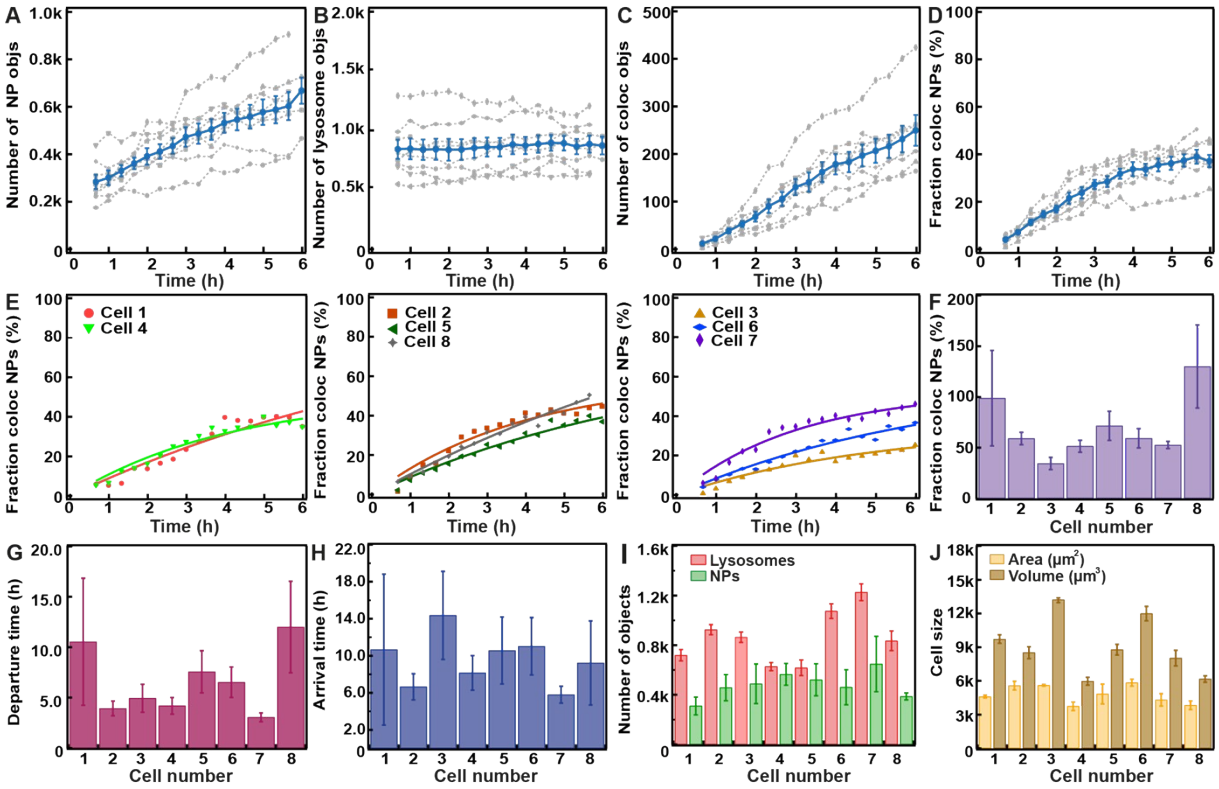

Supplementary Figure S8. Nanoparticle colocalization with lysosomes in HeLa cells exposed for 10 min to 300 µg/ml 100 nm nanoparticles in DMEM medium supplemented with 4 mg/ml human serum and stained with LysoTracker. Average number over all cells *(blue)* and for individual cells *(grey)* of ***(A)*** detected nanoparticle objects, ***(B)*** lysosome objects, ***(C)*** nanoparticle objects colocalized with lysosome objects and ***(D)*** fraction of nanoparticle objects colocalized with lysosome objects. The average results are the mean and standard error of the results obtained in 8 individual cells. ***(E)*** Fits of Eq. 2 *(solid line)* to the fraction of nanoparticle objects colocalized with lysosome objects *(symbols)* in individual cells. ***(F)*** Fraction of nanoparticle objects ultimately colocalized with lysosome objects (f_l) extracted from the fits to individual cells shown in E. ***(G)*** Departure time of nanoparticle objects from the membrane (τ) extracted from the fits to individual cells shown in E. ***(H)*** Lysosome arrival time of nanoparticle objects (τ_l) calculated from F and G. Error bars in panel F, G are uncertainties from the fit, while error bars in panel H are uncertainties propagated from those of f_l and τ using Gauss' formula. ***(I)*** Number of nanoparticle *(red)* and lysosome objects *(green)* detected in individual cells averaged over all time points. The average results are the mean and standard error of the results obtained for 17 time points. ***(J)*** Area *(yellow)* and volume *(brown)* of individual cells. z-stack images were acquired using a Zeiss LSM 880.

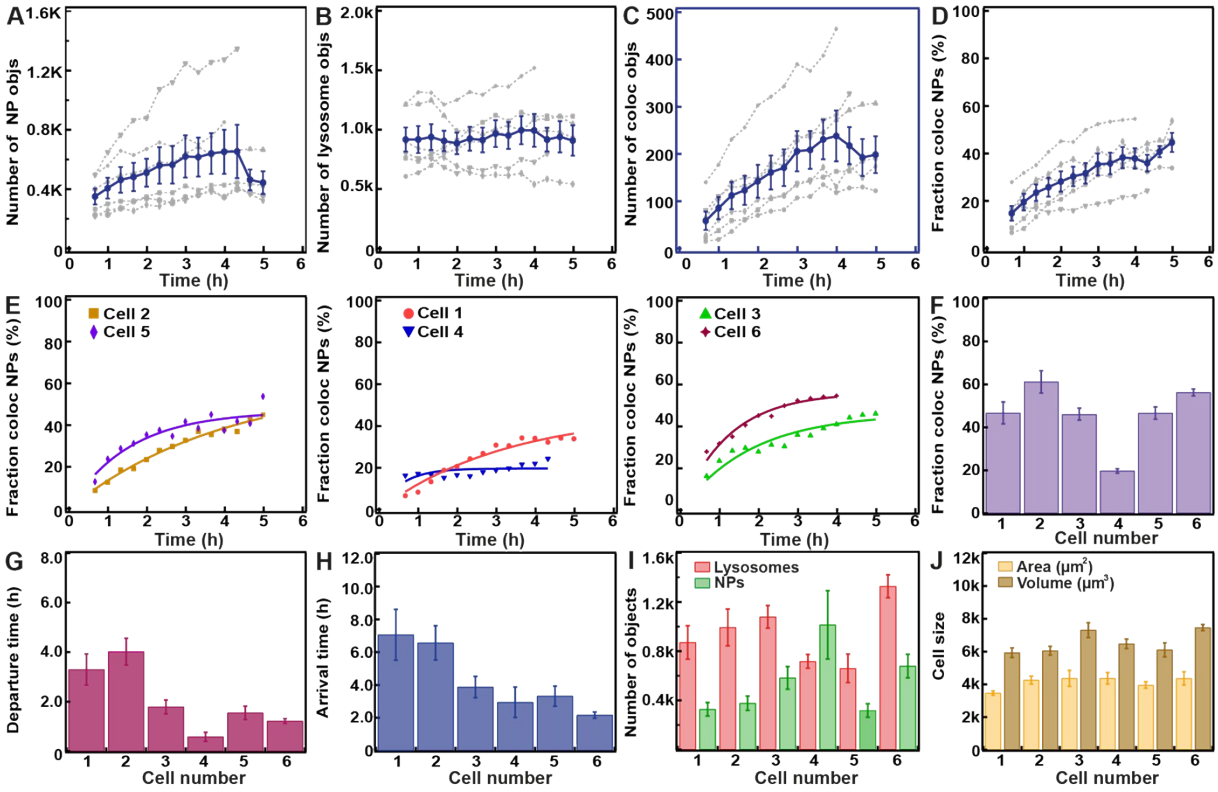

Supplementary Figure S9. Nanoparticle colocalization with lysosomes in HeLa cells exposed for 15 min to 1600 μg/ml 200 nm nanoparticles in DMEM medium supplemented with 4 mg/ml human serum and stained with LysoTracker. Average number over all cells *(dark blue)* and for individual cells *(grey)* of ***(A)*** detected nanoparticle objects, ***(B)*** lysosome objects, ***(C)*** nanoparticle objects colocalized with lysosome objects and ***(D)*** fraction of nanoparticle objects colocalized with lysosome objects. The average results are the mean and standard error of the results obtained in 6 individual cells. ***(E)*** Fits of Eq. 2 *(solid line)* to the fraction of nanoparticle objects colocalized with lysosome objects *(symbols)* in individual cells. ***(F)*** Fraction of nanoparticle objects ultimately colocalized with lysosome objects (f_l) extracted from the fits to individual cells shown in E. ***(G)*** Departure time of nanoparticle objects from the membrane (τ) extracted from the fits to individual cells shown in E. (***H)*** Lysosome arrival time of nanoparticle objects (τ_l) calculated from F and G. Error bars in panel F, G are uncertainties from the fit, while error bars in panel H are uncertainties propagated from those of f_l and τ using Gauss' formula. ***(I)*** Number of nanoparticle *(red)* and lysosome objects *(green)* detected in individual cells averaged over all time points. The average results are the mean and standard error of the results obtained over 14 time points. ***(J)*** Area *(yellow)* and volume *(brown)* of individual cells. z-stack images were acquired using a Zeiss LSM 880.

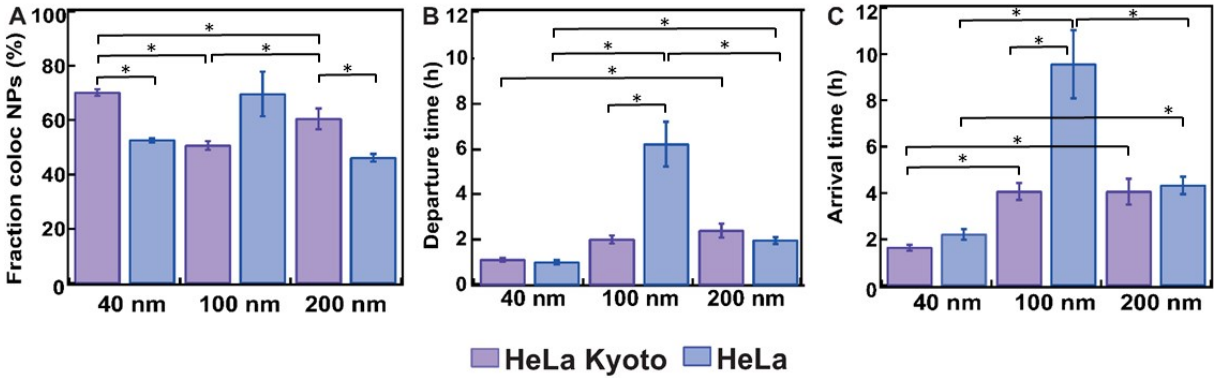

Supplementary Figure S10. Fitting parameters extracted from individual cell results and subsequently averaged over cells. HeLa and HeLa Kyoto cells were exposed to 40, 100 and 200 nm carboxylated polystyrene nanoparticles and stained with LysoTracker, then colocalization with the lysosomes was calculated (see Experimental section for details) and Equation (2) was fitted to the fraction of nanoparticle objects colocalized with lysosome objects as a function of time (Supplementary Fig. S4-S9). The resulting fitting parameters were then averaged over cells. Note the difference compared to Figure 4, where the colocalization was averaged and Equation (2) was fitted to this averaged data. ***(A)*** Fraction of nanoparticle objects ultimately colocalized with lysosome objects (f_l). ***(B)*** Typical departure time of nanoparticle objects from the membrane (τ). ***(C)*** Typical arrival time to lysosomes of nanoparticle objects (τ_l) calculated from A and B. HeLa Kyoto *(purple)* and HeLa cells *(blue)*. Error bars in panel A-B are uncertainties propagated from the uncertainties from the fits to the individual cell data using Gauss' formula, while error bars in panel C are uncertainties propagated from those from the individual cells using Gauss' formula which, in turn, were propagated from the uncertainties of the fits of the individual cell data in the same way. Significant differences (*) between the two cell types were assessed using a Mann-Whitney test; similarly, significant differences (*) between the three nanoparticle sizes were assessed using a Kruskal-Wallis test and, when significant, using a Conover pairwise multiple comparison test to identify the samples that differed. The results are comparable to those obtained by first averaging the results obtained for all individual cells and then fitting the model to the average, as shown in Figure 4D-F.

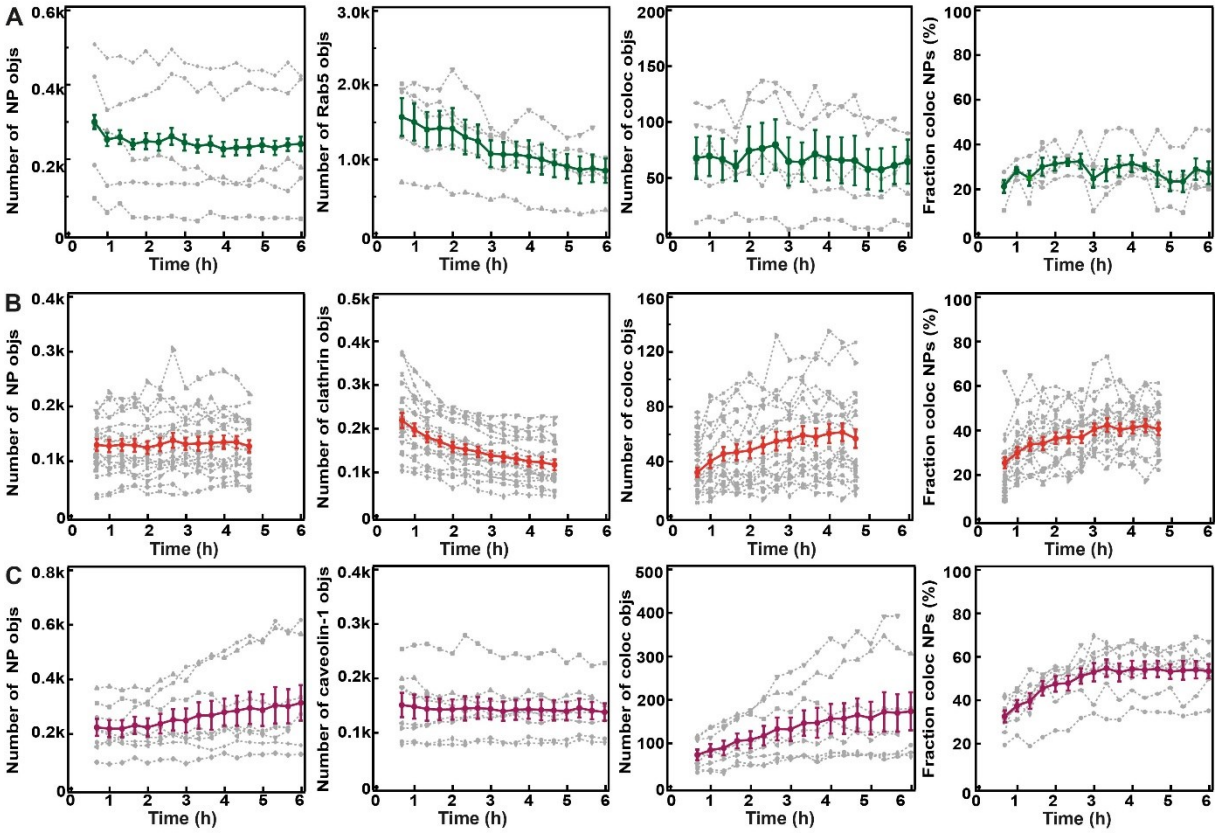

Supplementary Figure S11. Quantification of nanoparticle colocalization with Rab5, clathrin and caveolin-1 in HeLa Kyoto cells exposed to 100 nm carboxylated polystyrene nanoparticles. HeLa Kyoto cells expressing labelled Rab5, or clathrin or caveolin-1 were exposed for 10 min to 300 µg/ml 100 nm carboxylated polystyrene in DMEM medium supplemented with 4 mg/ml human serum. Then colocalization with the different markers was calculated as described in the Methods. From left to right: ***(A)*** Individual cell results *(grey)* and average number *(green)* of detected nanoparticle objects, Rab5 objects, number of nanoparticle objects colocalized with Rab5 objects and fraction of nanoparticle objects colocalized with Rab5 objects *(green).* (Mean± SE (n=5)). ***(B)*** Individual cell results *(grey)* and average number *(orange)* of detected nanoparticle objects, clathrin objects, number of nanoparticle objects colocalized with clathrin objects and fraction of nanoparticle objects colocalized with clathrin objects. (Mean± SE (n=20)). ***(C)*** Individual cell results *(grey)* and average number *(purple)* of detected nanoparticle objects, caveolin-1 objects, nanoparticle objects colocalized with caveolin-1 objects and fraction of nanoparticle objects colocalized with caveolin-1 objects (Mean± SE (n=8)). z-stacks images were acquired using a Zeiss LSM 880.

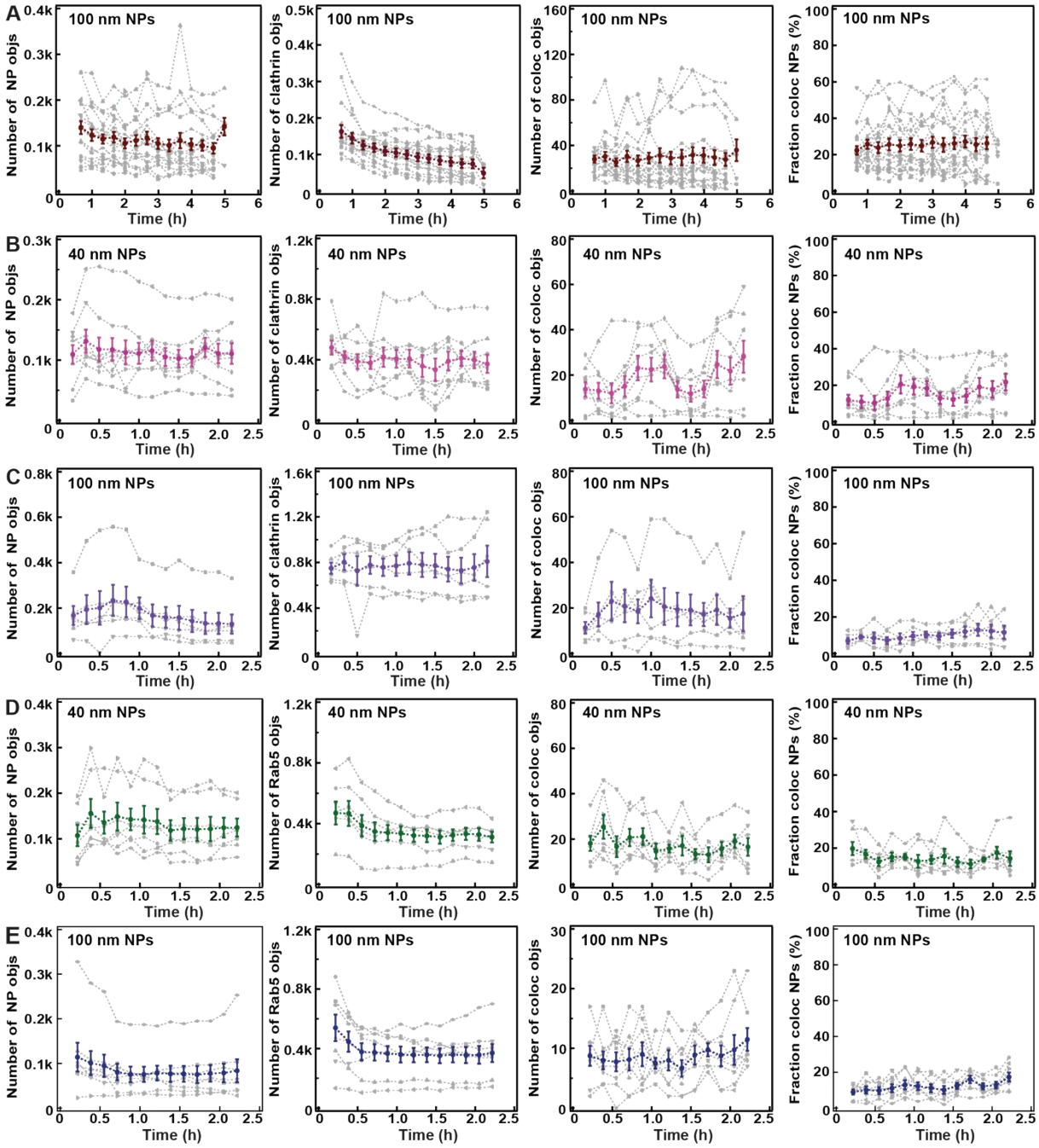

Supplementary Figure S12. Quantification of nanoparticle colocalization with clathrin and Rab5 on the "cell edges" of HeLa Kyoto cells exposed to 100 nm and 40 nm carboxylated polystyrene nanoparticles. HeLa Kyoto cells expressing labelled clathrin were exposed, respectively, for 10 min to 300 µg/ml of 100 nm and 5 min to 75 µg/ml of 40 nm carboxylated polystyrene nanoparticles in DMEM medium supplemented with 4 mg/ml human serum. The colocalization with proteins in the region closer to the cell membrane was calculated as described in the Methods. From left to right: ***(A)*** Individual cell results *(grey)* and average number *(brick)* of detected 100 nm nanoparticle objects, clathrin objects, nanoparticle objects colocalized with clathrin objects and fraction of nanoparticle objects colocalized with clathrin objects. (Mean± SE (n=20)) z-stacks were acquired using a Zeiss LSM 880. ***(B)*** Individual cell results *(grey)* and average number *(pink)* of detected 40 nm nanoparticle objects, clathrin objects, nanoparticle objects colocalized with clathrin objects and fraction of nanoparticle objects colocalized with clathrin objects. (Mean± SE (n=6)) ***(C)*** Individual

cell results *(grey)* and average number *(purple)* of detected 100 nm nanoparticle objects, clathrin objects, nanoparticle objects colocalized with clathrin objects and fraction of nanoparticle objects colocalized with clathrin objects. (Mean± SE (n=9)) ***(D)*** Individual cell results *(grey)* and average number *(green)* of detected 40 nm nanoparticle objects, Rab5 objects, nanoparticle objects colocalized with Rab5 objects and fraction of nanoparticle objects colocalized with Rab5 objects. (Mean± SE (n=7)) ***(E)*** Individual cell results *(grey)* and average number *(blue)* of detected 100 nm nanoparticle objects, Rab5 objects, nanoparticle objects colocalized with Rab5 objects and fraction of nanoparticle objects colocalized with Rab5 objects. (Mean± SE (n=8)) (B-E) z-stacks were acquired using a DeltaVision Elite and deconvoluted.

Supplementary Movie S1. Live-cell imaging as a tool for quantitative analysis of nanoparticle uptake and intracellular transport. Example raw 3D z-stack of images of a HeLa Kyoto cell stained with LysoTracker (*red)* and exposed to 300 µg/ml 100 nm carboxylated polystyrene nanoparticles *(green)* for a 10 min "pulse". Cell contours were manually defined based on the LysoTracker channel and a 3D cell mask was generated. The cell mask was applied to the nanoparticles and LysoTracker fluorescence channels defining the region of interest for analysis. Further images in both channels were segmented based on the mean intensity and homogeneous spherical nanoparticles *(green)* and lysosome *(red)* objects with fixed volume identified. The overlapped raw and segmented images are shown over a 5 h "chase" and were acquired every 20 min starting 40 min after exposure to nanoparticles (zero time point in the movie). In the same way segmented images with detected nanoparticle objects that colocalize with lysosomes *(yellow)* are shown. Images were acquired with a confocal LSM880 microscope in fast airy scan mode and processed in Imaris software.

Supplementary Movie S2. HeLa cell expressing LAMP1 exposed to 100 nm carboxylated polystyrene nanoparticles after 6 h chase. Example raw 2D images of a HeLa cell transfected with LAMP1-RFP plasmid (*red)* and exposed to 250 µg/ml 100 nm carboxylated polystyrene nanoparticles *(green)* for a 5 min "pulse". Images are shown over a 2 min time course and were acquired every 2 s starting after a 6 h "chase" (zero time point in the movie). Images were acquired with an epifluorescence DeltaVision Elite microscope and decovoluted with SoftWoRx software.

Supplementary Movie S3. HeLa cell exposed to 100 nm carboxylated polystyrene nanoparticles and stained with LysoTracker after a 19 h chase. Example raw 2D images of a HeLa cell stained with Lysotracker (*red)* and exposed to 400 µg/ml 100 nm carboxylated polystyrene nanoparticles *(green)* for a 10 min "pulse". Images are shown over a 5 min time course and were acquired every 2 s starting after a 19 h "chase" (zero time point in the movie). Images were acquired with an epifluorescence DeltaVision Elite microscope and deconvoluted with SoftWoRx software.

Supplementary Movie S4. Overexpression limits: HeLa Kyoto cell expressing clathrin stained with LysoTracker and exposed to 40 nm carboxylated polystyrene nanoparticles. Example raw 2D images of a HeLa Kyoto cell transfected with mRFP-Clc plasmid *(red)*, stained with LysoTracker *(green)* and exposed to 100 µg/ml 40 nm carboxylated polystyrene nanoparticles *(blue)* for a 10 min "pulse". Images are shown over a 3 min time course and were acquired every 2 s starting after a 6 h "chase" (zero time point in the movie). Images were acquired with a confocal LSM880 microscope in fast airy scan mode.

Supplementary Movie S5. HeLa Kyoto cell expressing clathrin exposed to 100 nm carboxylated polystyrene nanoparticles. Example raw 2D images of a HeLa Kyoto cell transfected with mRFP-Clc plasmid *(red)* and exposed to 500 µg/ml 100 nm carboxylated polystyrene nanoparticles *(green)* for a 10 min "pulse". Images are shown over a 2 min "chase" and were acquired every second starting immediately after exposure to nanoparticles (zero time point in the movie). Images were acquired with a confocal LSM880 microscope in fast airy scan mode.

Supplementary Movie S6. HeLa Kyoto cell expressing caveolin exposed to 100 nm carboxylated polystyrene nanoparticles. Example raw 2D images of a HeLa Kyoto cell transfected with CAV1-mEGFP plasmid *(green)* and exposed to 500 µg/ml

100 nm carboxylated polystyrene nanoparticles *(red)* for a 10 min “pulse”. Images are shown over a 1 h “chase” and were acquired every 1.5 min starting immediately after exposure to nanoparticles (zero time point in the movie). Images were acquired with a confocal LSM880 microscope in fast airy scan mode.

Supplementary Movie S7. Micropinocytosis in HeLa Kyoto cell exposed to 100 nm carboxylated polystyrene nanoparticles. Example raw 2D images of a HeLa Kyoto cell transfected with pMyrPalm-mEGFP plasmid *(green)* and exposed to 500 µg/ml 100 nm carboxylated polystyrene nanoparticles *(red)* for a 10 min “pulse”. Images are shown over a 1.5 min “chase” and were acquired every second starting immediately after exposure to nanoparticles (zero time point in the movie). Images were acquired with a confocal LSM880 microscope in fast airy scan mode.

Supplementary Movie S8. HeLa Kyoto cell expressing Rab5 exposed to 100 nm carboxylated polystyrene nanoparticles. Example raw 2D images of a HeLa Kyoto cell transfected with Rab5-GFP plasmid (*green)* and exposed to 400 µg/ml 100 nm carboxylated polystyrene nanoparticles *(red)* for a 5 min “pulse”. Images are shown over a 17 min “chase” and were acquired every 5 s starting immediately after exposure to nanoparticles (zero time point in the movie). Images were acquired with a confocal LSM880 microscope in fast airy scan mode.

Supplementary Movie S9. HeLa Kyoto cell expressing EEA1 exposed to 100 nm carboxylated polystyrene nanoparticles. Example raw 2D images of a HeLa Kyoto cell transfected with ctEEA1-GFP plasmid *(green)* and exposed to 250 µg/ml 100 nm carboxylated polystyrene nanoparticles *(red)* for a 5 min “pulse”. Images are shown over a 13 min “chase” and were acquired every 20 s starting immediately after exposure to nanoparticles (zero time point in the movie). Images were acquired with a confocal LSM880 microscope in fast airy scan mode.

References

1. T. Bergeland, L. Haugen, O. J. B. Landsverk, H. Stenmark and O. Bakke, *EMBO Rep*, 2008, **9**, 171-178.
2. P. Steigemann, C. Wurzenberger, M. H. A. Schmitz, M. Held, J. Guizetti, S. Maar and D. W. Gerlich, *Cell*, 2009, **136**, 473-484.
3. N. M. Sherer, M. J. Lehmann, L. F. Jimenez-Soto, A. Ingmundson, S. M. Horner, G. Cicchetti, P. G. Allen, M. Pypaert, J. M. Cunningham and W. Mothes, *Traffic*, 2003, **4**, 785-801.
4. J.-F. Gilles, M. Dos Santos, T. Boudier, S. Bolte and N. Heck, *Methods*, 2017, **115**, 55-64.
5. C. Röcker, M. Pötzl, F. Zhang, W. J. Parak and G. U. Nienhaus, *Nature Nanotechnology*, 2009, **4**, 577-580.
6. X. Jiang, S. Weise, M. Hafner, C. Röcker, F. Zhang, W. J. Parak and G. U. Nienhaus, *J R Soc Interface*, 2010, **7 Suppl 1**, S5-S13.
7. S. Milani, F. Baldelli Bombelli, A. S. Pitek, K. A. Dawson and J. Rädler, *ACS Nano*, 2012, **6**, 2532-2541.